



Porter Goff, K., Nicol, D., Williams, C., Crump, M., Zieleniewski, F., Samphire, J., Baker, E., & Woolfson, D. (2019). Stabilizing and Understanding a Miniprotein by Rational Redesign. *Biochemistry*, 58(28), 3060-3064. <https://doi.org/10.1021/acs.biochem.9b00067>

Peer reviewed version

Link to published version (if available):  
[10.1021/acs.biochem.9b00067](https://doi.org/10.1021/acs.biochem.9b00067)

[Link to publication record in Explore Bristol Research](#)  
PDF-document

This is the author accepted manuscript (AAM). The final published version (version of record) is available online via ACS Publications at <https://pubs.acs.org/doi/10.1021/acs.biochem.9b00067>. Please refer to any applicable terms of use of the publisher.

## University of Bristol - Explore Bristol Research

### General rights

This document is made available in accordance with publisher policies. Please cite only the published version using the reference above. Full terms of use are available:  
<http://www.bristol.ac.uk/red/research-policy/pure/user-guides/ebr-terms/>



Porter Goff, K., Nicol, D., Williams, C., Crump, M., Zieleniewski, F., Samphire, J., ... Woolfson, D. (2019). Stabilizing and Understanding a Miniprotein by Rational Redesign. *Biochemistry*, 58(28), 3060-3064. [9b00067]. <https://doi.org/10.1021/acs.biochem.9b00067>

Link to published version (if available):

[10.1021/acs.biochem.9b00067](https://doi.org/10.1021/acs.biochem.9b00067)

[Link to publication record in Explore Bristol Research](#)

PDF-document

## **University of Bristol - Explore Bristol Research**

### **General rights**

This document is made available in accordance with publisher policies. Please cite only the published version using the reference above. Full terms of use are available:  
<http://www.bristol.ac.uk/pure/about/ebr-terms>

# Stabilizing and Understanding a Miniprotein by Rational Redesign

Kathryn L. Porter Goff,<sup>†</sup> Debbie Nicol,<sup>†</sup> Christopher Williams,<sup>†,‡</sup> Matthew P. Crump,<sup>†,‡</sup> Francis Zieleniewski,<sup>†</sup> Jennifer L. Samphire,<sup>†</sup> Emily G. Baker,<sup>†</sup> Derek N. Woolfson<sup>\*,†,‡,§</sup>

<sup>†</sup> School of Chemistry, University of Bristol, Cantock's Close, Bristol BS8 1TS, UK

<sup>‡</sup> BrisSynBio, University of Bristol, Life Sciences Building, Tyndall Avenue, Bristol, BS8 1TQ, UK

<sup>§</sup> School of Biochemistry, University of Bristol, Medical Sciences Building, University Walk, Bristol BS8 1TD, UK

## Supporting Information Placeholder

**ABSTRACT:** Miniproteins reduce the complexity of the protein-folding problem allowing systematic studies of contributions to protein folding and stabilization. Here, we describe the rational redesign of a miniprotein, PP $\alpha$ , comprising a polyproline-II helix, loop and  $\alpha$  helix. The redesign provides a *de novo* framework to interrogate non-covalent interactions. Optimized PP $\alpha$  has significantly improved thermal stability with a midpoint unfolding temperature ( $T_M$ ) of 51 °C. Its NMR structure indicates a higher density of stabilizing non-covalent interactions than the parent peptide, specifically increased CH- $\pi$  interactions. In part, we attribute this to improved long-range electrostatic interactions between the two helical elements. We probe further sequence-to-stability relationships in the miniprotein through a series of rational mutations.

The primary sequence of a protein determines its three-dimensional structure and function. Understanding sequence-to-structure relationships is known as the protein-folding problem.<sup>1</sup> Studying miniproteins reduces the complexity of the problem, allowing contributions to protein folding and stability to be dissected more easily.<sup>2, 3</sup> Prominent examples of miniproteins include: the Trp-cage,<sup>4</sup>  $\beta\alpha\beta$  motifs,<sup>5</sup> villin headpiece,<sup>6</sup> pancreatic peptides<sup>7-10</sup> and the Trp-Plexus.<sup>11</sup> The formation of many weak and cooperative non-covalent interactions is central to protein stability, allowing the loss of conformational entropy upon folding to be overcome. This is particularly important for miniproteins with fewer interactions possible.<sup>12</sup>

$\alpha$  Helices are common building blocks in proteins. They are often stabilized by tertiary and quaternary interactions, as exemplified in  $\alpha$ -helical coiled coils, a ubiquitous folding motif comprising two or more  $\alpha$  helices supercoiled around each other.<sup>13</sup> Most coiled-

coil sequences have a seven-residue heptad repeat, **abcdefg**, with hydrophobic residues at **a** and **d**, and polar residues at the remaining sites. This pattern leads to the association of helices *via* “knobs-into-holes” packing interactions, where side chains of one helix dock into diamond-shaped holes of another.<sup>14, 15</sup>  $\alpha$  Helices can also be stabilized by the interdigitation of proline (Pro, P) from polyproline-II helices between aromatic residues on  $\alpha$  helices, which are analogous to knobs-into-holes packing.<sup>2, 7, 16</sup>

Elsewhere, we describe the fragment-based design of a 34-residue miniprotein, PP $\alpha$ .<sup>17</sup> This comprises a polyproline-II helix, loop and  $\alpha$  helix adapted from natural proteins (Figure 1A,B).<sup>7, 16</sup> PP $\alpha$  is monomeric in aqueous solution and unfolds reversibly with a  $T_M$  of 39 °C. A solution NMR structure shows the stabilizing effect of Pro and tyrosine (Tyr, Y) interdigitation and associated CH- $\pi$  interactions. In the latter, protons of C-H bonds interact with aromatic rings.<sup>17-20</sup> Here, we explore the optimization of PP $\alpha$  by rational redesign, revealing sequence-to-stability relationships for the miniprotein fold and delivering a *de novo* framework of significantly enhanced thermal stability.

In the design of  $\alpha$ -helical coiled coils, charged residues often flank the hydrophobic core and form inter-helical Coulombic interactions.<sup>2</sup> We reasoned that PP $\alpha$  might be stabilized by introducing similar interactions between the **2** and **3** positions of the polyproline-II helix and the **e** and **g** positions of the  $\alpha$  helix (Figure 1A,C).

There are two extreme possibilities for pairing charged residues in PP $\alpha$ : a lysine (Lys, K)-based polyproline-II helix and a glutamic acid (Glu, E)-based  $\alpha$  helix or *vice versa* (PP $\alpha$ -KE and PP $\alpha$ -EK, respectively, Table 1). We optimized helix propensity for the solvent-exposed face of the  $\alpha$  helix by placing alanine (Ala, A) at **b** and **c** and Lys at **f** in both designs.

Otherwise, the helix-helix interface was maintained, with Pro at **1**, leucine (Leu, L) at **a** and Tyr at **d**, along with the PP $\alpha$  loop. We adopted the coiled-coil heptad nomenclature for the  $\alpha$ -helical sequence as it has a 7-residue repeat.

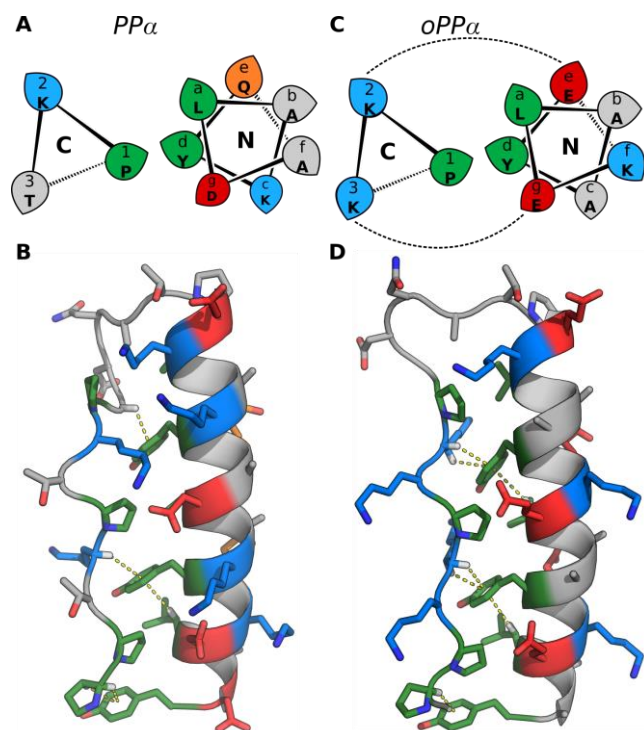


**Figure 1.** Helical wheel representations for the two helices in PP $\alpha$  (A) and PP $\alpha$ -KE (oPP $\alpha$ ) (C). Leaf tips indicate the direction of the C $\alpha$ -C $\beta$  bond vectors. Lowercase letters on the  $\alpha$  helix and numbers on the polyproline-II helix denote the helical register. C and N refer to the helix termini nearest the viewer. Dashed black lines: long-range interhelical electrostatic interactions. Representative models from the NMR ensembles of PP $\alpha$  (B, PDB entry 5LO2, model 14) and PP $\alpha$ -KE (D, PDB entry 6GWX, model 8). Dashed yellow lines: CH- $\pi$  interactions. Key: Lys (blue), Glu/Asp (red), and Tyr/Pro/Leu (green), Gln (orange).

PP $\alpha$ -KE and PP $\alpha$ -EK were synthesized by solid-phase peptide synthesis, purified by reverse-phase HPLC, and confirmed by MALDI-TOF mass spectrometry (Figure S1A,B). Circular dichroism (CD) spectroscopy revealed both peptides were 50%  $\alpha$  helical at 5 °C like PP $\alpha$  (Figure 2A). Sedimentation equilibrium analytical ultracentrifugation (AUC) showed that both peptides were monomeric (Figure S3A,B). PP $\alpha$ -KE had cooperative and reversible thermal unfolding transitions when followed by far- and near-UV CD (Figure S2U,V), and the T<sub>M</sub> (51 °C) was substantially increased over PP $\alpha$  (39 °C). However, PP $\alpha$ -EK was less stable than PP $\alpha$ -KE by 10 °C (Figure 2B). We posit that the reduced stability of PP $\alpha$ -EK stems from the large

charge on the  $\alpha$  helix—+6 compared to -2 for PP $\alpha$ -KE—and different propensities of Glu and Lys for  $\alpha$  and polyproline-II helices (Table S1,2).<sup>21,22</sup>

High-resolution NMR spectroscopy was used to determine the solution-phase structure of PP $\alpha$ -KE (Figure 1D), with 95.8% of the <sup>1</sup>H NMR resonances assigned. The core of the structure was well defined, while several of the solvent-exposed residues were more dynamic. The root-mean-square deviations (RMSDs) across the 20 structures of the ensemble were 0.52 ± 0.13 Å (backbone) and 1.05 ± 0.15 Å (all atom), comparable to those for the structure of PP $\alpha$  (Table S3).<sup>17</sup> A representative structure matched PP $\alpha$  with backbone and all-atom RMSDs of 0.5 Å and 0.9 Å, respectively.

The average distances between N $\epsilon$  of Lys and C $\delta$  of Glu introduced in PP $\alpha$ -KE were 8.7 ± 1.8 Å and 11.5 ± 2.4 Å for **2:e** and **3:g**, respectively. These fall outside of any accepted definition of salt-bridge interactions,<sup>23</sup> suggesting longer-range electrostatic interactions may stabilize the folded state of PP $\alpha$ -KE. To test this, the thermal stability of PP $\alpha$ -KE was measured at different salt concentrations in phosphate buffer (Figure S2C,D). With increased concentrations of NaCl from 0 to 700 mM the T<sub>M</sub> fell from 61 to 57 °C (Figure S2W), indicative of an electrostatic component to thermostability.

As PP $\alpha$  is stabilized by CH- $\pi$  interactions,<sup>17</sup> we searched for these in PP $\alpha$ -KE. This revealed 87 CH- $\pi$  interactions across the ensemble (4.35 per structure), an increase over PP $\alpha$  (68 CH- $\pi$  interactions; 3.4 per structure) (Figure 1B,D, Table S5 and Figure S8). A shift in CH donors between the two miniproteins was also observed. In PP $\alpha$ -KE fewer CH donors emanated from Pro residues (PP $\alpha$ -KE, 5; PP $\alpha$ , 22), but more arose from Leu (PP $\alpha$ -KE, 25; PP $\alpha$ , 4) and Lys residues (PP $\alpha$ -KE, 57; PP $\alpha$ , 15). On closer inspection, the side chains of Lys4 and Lys7 of PP $\alpha$ -KE lie across the faces of Tyr27 and Tyr20, respectively, leading to CH- $\pi$  interactions between the C $\alpha$  and C $\beta$  protons of the former and the aromatic rings of the latter. To test for CH- $\pi$  interactions experimentally, we replaced all of the electron-rich Tyr residues in PP $\alpha$ -KE by more-electron-poor phenylalanine (Phe, F) giving PP $\alpha$ -KE-Phe (Table 1). As with PP $\alpha$ ,<sup>17</sup> this reduced the T<sub>M</sub> by approximately 20 °C (Figure S2E,F). This indicates that CH- $\pi$  interactions are at play in PP $\alpha$ -KE in addition to van der Waals' forces.

Overall, we posit that the improved stability of PP $\alpha$ -KE arises from increased long-range electrostatic interactions between the polyproline-II and  $\alpha$  helix,<sup>24-27</sup> which lead to an increased density of shorter-range CH- $\pi$  interactions.

Tyr residues at the **d** sites of the 7-residue repeats of PPα and related natural folds are critical for folding and stability.<sup>7, 16, 17</sup> These residues form two vertices of 4-residue ‘holes’ defined by side chains at successive **d**, **a**, **g**, and **d** sites, which accommodate Pro ‘knobs’ from the polyproline-II helix. In PPα and PPα-KE, the **g** site is fixed as aspartic acid (Asp, D) or Glu,

respectively. The **a** sites are all Leu, which is the preferred residue in natural sequences.<sup>7, 28</sup> To explore possible substitutes for Leu at **a**, we made mutants with all three **a** sites replaced by: β-branched, isoleucine (Ile, I) or valine (Val, V); charged,

**Table 1. Designed peptides and summary of biophysical data.**

Peptide	Sequence and helical register	TM / °C	AUC *
	<i>321321321321321</i> <i>efgabcd efgabcd efgabcd efgabcd efgabcd</i>		
Parent PPα	PPTKPTKP GDNAT PEKLAKY QADLAKY QKDLADY	39	0.9
PPα-KE/oPPα	PPKKPKKP GDNAT PEKLAAY EKELAAY EKELAAY	51	1.0
PPα-EK	PP <b>EEPEEP</b> GDNAT PEKLAAY <b>KKKLAAY</b> <b>KKKLAAY</b>	40	0.9
PPα-KE-Phe	PPKKPKKP GDNAT PEKLA <b>AF</b> EKELA <b>AF</b> EKELA <b>AF</b>	33	1.0
PPα-KE-E@a	PPKKPKKP GDNAT PEK <b>E</b> AAY EKE <b>E</b> AAY EKE <b>E</b> AAY	-	-
PPα-KE-A@a	PPKKPKKP GDNAT PEK <b>A</b> AAY EKE <b>A</b> AAY EKE <b>A</b> AAY	-	1.0
PPα-KE-K@a	PPKKPKKP GDNAT PEK <b>K</b> AAY EKE <b>K</b> AAY EKE <b>K</b> AAY	19	1.0
PPα-KE-I@a	PPKKPKKP GDNAT PEK <b>I</b> AAY EKE <b>I</b> AAY EKE <b>I</b> AAY	40	1.0
PPα-KE-V@a	PPKKPKKP GDNAT PEK <b>V</b> AAY EKE <b>V</b> AAY EKE <b>V</b> AAY	34	1.0
PPα-KE-A@g	PPKKPKKP GDNAT PEKLA <b>EY</b> EKALA <b>EY</b> EKALA <b>EY</b>	21	1.0
PPα-KE-L@g	PPKKPKKP GDNAT PEKLA <b>EY</b> EKLLA <b>EY</b> EKLLA <b>EY</b>	76	1.2
PPα-KE-a↔g	PPKKPKKP GDNAT PEKLAAY <b>A</b> ALE <b>KEY</b> <b>A</b> ALE <b>KEY</b>	19	1.1
oPPα-2	PPKKP GDNAT PEKLAAY EKELAAY	19	0.9
oPPα-4	PPKKPKKP <b>PKKP</b> GDNAT PEKLAAY EKELAAY EKELAAY EKELAAY	66	1.0
oPPα-5	PPKKPKKP <b>PKKP</b> PKKP GDNAT PEKLAAY EKELAAY EKELAAY EKELAAY EKELAAY	72	1.0
oPPα-5-skip	PPKKPKKP <b>PKKP</b> PKKP GDNAT PEKLAAY EKELAAY EKELAAY EKELAAY EKELAAY	68	1.0

Peptides were capped with N-terminal acetyl and C-terminal amide groups. \*Oligomeric state (× monomer mass) as determined by AUC. Mutations to the PPα-KE/oPPα interface are shown in bold.

Glu or Lys; or Ala (Table 1).

AUC confirmed that these PPα-KE-X@a mutants were monomeric in solution (Figure S3). However, CD spectroscopy revealed a range of stabilities. PPα-KE-E@a was not folded, possibly due to the proximal glutamates at **e** if the α helix were folded. The stabilities of PPα-KE-A@a and PPα-KE-K@a were compromised compared to PPα-KE (Figure 2C,D). By contrast, both PPα-KE-I@a and PPα-KE-V@a were folded, albeit with reduced thermal stabilities compared with PPα-KE. This suggests that the extra steric bulk of the β carbon may hinder docking of Pro into the hole, although we note that α-helical propensities of both Ile and Val are also lower than that of Leu.<sup>21</sup>

We also probed the **g** position of the hole, initially *via* an Ala mutation to determine the contribution of this residue to stability. To maintain the introduced electrostatic interactions between the helices, Glu was shifted to the **c** position, although this may introduce

favorable K<sub>i</sub>→E<sub>i+4</sub> interactions. The resulting PPα-KE-A@g was monomeric, but significantly less stable than PPα-KE (Figure S2I,J). Next, we mutated the **g** position to Leu, giving a fully hydrophobic hole. The thermal unfolding transition of PPα-KE-L@g was broad, with a T<sub>M</sub> of 76 °C (Figure S2K,L). However, the CD signal was concentration dependent, indicating aggregation (Figure S2M,N). AUC experiments returned a mass of 1.2 × monomer mass, suggesting PPα-KE-L@g forms higher-order species, which could involve the wider hydrophobic interface. Our interests lie in fully monomeric miniproteins, so the **g** positions were not probed further.

As a final exploration of hole-residue preferences, we swapped the **a** and **g** residues (PPα-KE-a↔g). This tests an alternate helical register, LXXYXXX, as opposed to LXXYXXX in PPα-KE. Residues at **e** and **c**, and **b** and **f** were swapped to avoid introducing charged interactions in the α helix of PPα-KE-a↔g not present

in PP $\alpha$ -KE. PP $\alpha$ -KE- $\alpha\leftrightarrow g$  was less folded and less thermally stable ( $T_M$  19 °C) than PP $\alpha$ -KE. Thus, PP $\alpha$ -KE possesses the optimal arrangement of residues in the diamond-shaped hole.

The results of this mutagenesis study reveal that Leu at **a**, Tyr at **d** and Glu at **g** provide the optimal 'hole' to accommodate Pro in PP $\alpha$ -like miniproteins. On this basis, we renamed PP $\alpha$ -KE as optimised-PP $\alpha$ , oPP $\alpha$ .

Using oPP $\alpha$ , we investigated the effect of helix length on stability. Variants were synthesised with 1-, 3- and 4-unit polyproline-II-helical repeats and corresponding 2-, 4- and 5- heptad  $\alpha$ -helical repeats (Table 1, Figure S15). Like oPP $\alpha$ , which completes this series with two polyproline-II and three

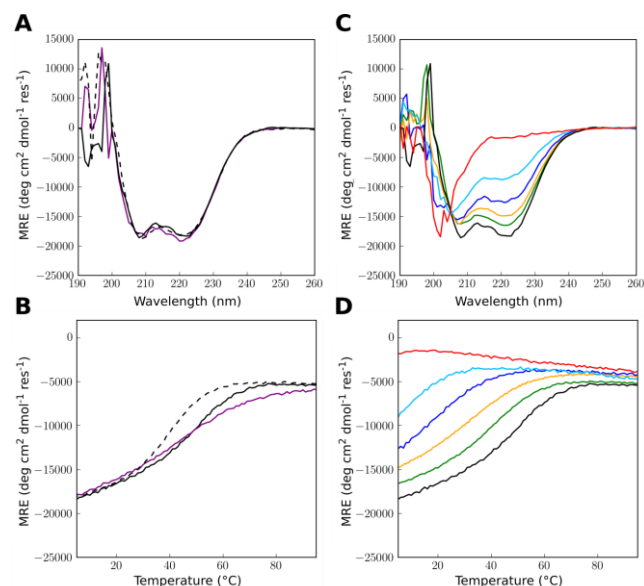


**Figure 2.** Folding and stability of PP $\alpha$ -KE and mutants. Far-UV CD spectra at 5 °C for: (A) parent PP $\alpha$  (black, dash), PP $\alpha$ -KE (black), and PP $\alpha$ -EK (purple); and (C) PP $\alpha$ -KE-E@a (red), PP $\alpha$ -KE-A@a (sky blue), PP $\alpha$ -KE-K@a (blue), PP $\alpha$ -KE-I@a (green), PP $\alpha$ -KE-V@a (orange), and PP $\alpha$ -KE (black). (B&D) Temperature dependence of the mean residue ellipticity (MRE) at 222 nm, with the key as for panels A&C. Conditions: 100  $\mu$ M peptide, PBS, pH 7.4.

$\alpha$ -helical repeats, these peptides were monomers (Figure S3M,N,O). However, only oPP $\alpha$ , oPP $\alpha$ -4 and oPP $\alpha$ -5 were appreciably and stably folded (Figure 3), with the  $T_M$  increasing from 51 to 66 to 72 °C, respectively. As observed in  $\alpha$ -helical coiled coils, folding and stability increases in a non-linear, cooperative manner.<sup>29, 30</sup>

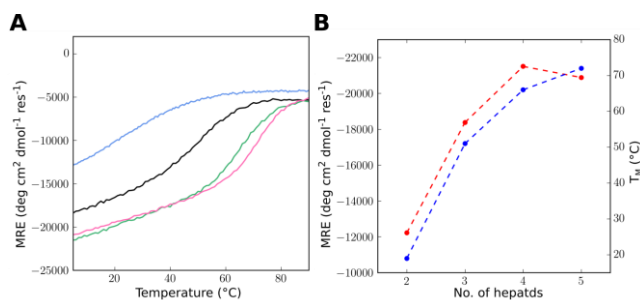


**Figure 3.** Folding and stability of oPP $\alpha$  variants of different lengths. (A) Thermal unfolding curves for oPP $\alpha$ -2 (blue), oPP $\alpha$  (black), oPP $\alpha$ -4 (green), and oPP $\alpha$ -5 (pink). (B) Plot of heptad length vs  $T_M$  (blue) and MRE<sub>222</sub> at 5 °C (red). Conditions: 100  $\mu$ M peptide, PBS, pH 7.4.

There is a periodicity mismatch between the 3- and 7- residue sequence repeats of polyproline-II and  $\alpha$  helices: the former span  $\approx$  9.3 Å and the latter  $\approx$  10.5 Å. For oPP $\alpha$ -5 this could result in a  $\approx$  6 Å discrepancy over the lengths of the helices in the interface. The bacterial adhesin AgI/II from *S. mutans* overcomes this with Pro insertions that break the PXX repeat.<sup>16</sup> Therefore, we introduced an extra Pro to the middle of the polyproline-II repeat of oPP $\alpha$ -5. This peptide, oPP $\alpha$ -5-skip, was monomeric, folded and stable (Figure S2S,T) but had a slightly lower  $T_M$  than the parent. This suggests that the helix-helix interface of the oPP $\alpha$  fold is plastic and accommodates minor mismatches in periodicities, perhaps not possible for longer, fibrous assemblies.

In summary, a miniprotein fold has been optimized by rational protein redesign to give oPP $\alpha$ , a completely *de novo* framework with significantly enhanced thermal stability relative to the parent design. We propose that complementary long-range electrostatic interactions and increased shorter-range non-covalent interactions are responsible for the enhanced stability. The specific sequence-to-structure/stability relationships that we have explored should help guide further designs of PP $\alpha$ -like miniproteins. oPP $\alpha$  should be a useful addition to the toolkit of synthetic peptide building blocks for constructing more-complex systems through modular assembly.<sup>31, 32</sup>

## ASSOCIATED CONTENT

### Supporting Information

The Supporting Information is available free of charge on the ACS Publications website.

Experimental details and characterization data.

## AUTHOR INFORMATION

### Corresponding Author

\*d.n.woolfson@bristol.ac.uk



## ORCID

Kathryn L. Porter Goff: 0000-0002-0533-7791  
Debbie Nicol: 0000-0001-6160-659X  
Christopher Williams: 0000-0001-5806-9842  
Matthew P. Crump: 0000-0002-7868-5818  
Francis Zieleniewski: 0000-0003-1529-8594  
Jennifer L. Samphire: 0000-0002-5945-415X  
Emily G. Baker: 0000-0002-1593-5525  
Derek N. Woolfson: 0000-0002-0394-3202

## Funding

KLPG, DN, JLS and FZ are funded by the EPSRC-funded Bristol Chemical Synthesis Centre for Doctoral Training (EP/G036764/1). EGB and DNW are supported by a European Research Council Advanced Grant (340764). CW and the 700 MHz NMR spectrometer are supported by BrisSynBio, a BBSRC/EPSC-fund Synthetic Biology Research Centre (BB/L01386X1). DNW holds a Royal Society Wolfson Research Merit Award (WM140008). We thank the reviewers of the original manuscript for insightful comments.

## Notes

The authors declare no competing financial interest.

## REFERENCES

- (1) Dill, K. A., Ozkan, S. B., Shell, M. S., and Weikl, T. R. (2008) The protein folding problem., *Annu. Rev. Biophys.* 37, 289-316.
- (2) Baker, E. G., Bartlett, G. J., Porter Goff, K. L., and Woolfson, D. N. (2017) Miniprotein Design: Past, Present, and Prospects., *Acc. Chem. Res.* 50, 2085-2092.
- (3) Gelman, H., and Gruebele, M. (2014) Fast protein folding kinetics., *Q. Rev. Biophys.* 47, 95-142.
- (4) Neidigh, J. W., Fesinmeyer, R. M., and Andersen, N. H. (2002) Designing a 20-residue protein., *Nat. Struct. Biol.* 9, 425-430.
- (5) Liang, H. H., Chen, H., Fan, K. Q., Wei, P., Guo, X. R., Jin, C. W., Zeng, C., Tang, C., and Lai, L. H. (2009) De novo design of a  $\beta\alpha\beta$  motif., *Angew. Chem. Int. Ed.* 48, 3301-3303.
- (6) McKnight, C. J., Matsudaira, P. T., and Kim, P. S. (1997) NMR structure of the 35-residue villin headpiece subdomain., *Nat. Struct. Biol.* 4, 180-184.
- (7) Blundell, T. L., Pitts, J. E., Tickle, I. J., Wood, S. P., and Wu, C. W. (1981) X-ray analysis (1.4-Å resolution) of avian pancreatic polypeptide: Small globular protein hormone., *Proc. Natl. Acad. Sci. USA* 78, 4175-4179.
- (8) Chin, J. W., and Schepartz, A. (2001) Concerted evolution of structure and function in a miniature protein., *J. Am. Chem. Soc.* 123, 2929-2930.
- (9) Hodges, A. M., and Schepartz, A. (2007) Engineering a monomeric miniature protein., *J. Am. Chem. Soc.* 129, 11024-11025.
- (10) Zondlo, N. J., and Schepartz, A. (1999) Highly specific DNA recognition by a designed miniature protein., *J. Am. Chem. Soc.* 121, 6938-6939.
- (11) Craven, T. W., Cho, M. K., Traaseth, N. J., Bonneau, R., and Kirshenbaum, K. (2016) A miniature protein stabilized by a cation- $\pi$  interaction network., *J. Am. Chem. Soc.* 138, 1543-1550.
- (12) Pace, C. N., Scholtz, J. M., and Grimsley, G. R. (2014) Forces stabilizing proteins., *FEBS Lett.* 588, 2177-2184.
- (13) Woolfson, D. N. (2017) Coiled-coil design: updated and upgraded., *Subcell. Biochem.* 82, 35-61.
- (14) Crick, F. H. (1953) The packing of alpha-helices: simple coiled coils., *Acta Crystallogr.* 6, 689-697.
- (15) Walshaw, J., and Woolfson, D. N. (2001) SOCKET: a program for identifying and analysing coiled-coil motifs within protein structures., *J. Mol. Biol.* 307, 1427-1450.
- (16) Larson, M. R., Rajashankar, K. R., Patel, M. H., Robinette, R. A., Crowley, P. J., Michalek, S., Brady, L. J., and Deivanayagam, C. (2010) Elongated fibrillar structure of a streptococcal adhesin assembled by the high-affinity association of  $\alpha$ - and PPII-helices, *Proc. Natl. Acad. Sci. USA* 107, 5983-5988.
- (17) Baker, E. G., Williams, C., Hudson, K. L., Bartlett, G. J., Heal, J. W., Porter Goff, K. L., Sessions, R. B., Crump, M. P., and Woolfson, D. N. (2017) Engineering protein stability with atomic precision in a monomeric miniprotein., *Nat. Chem. Biol.* 13, 764-770.
- (18) Kang, Y. K., and Byun, B. J. (2012) Strength of CH $\cdots\pi$  interactions in the C-terminal subdomain of villin headpiece., *Biopolymers* 97, 778-788.
- (19) Nishio, M., Umezawa, Y., Fantini, J., Weiss, M. S., and Chakrabarti, P. (2014) CH- $\pi$  hydrogen bonds in biological macromolecules., *Phys. Chem. Chem. Phys.* 16, 12648-12683.
- (20) Zondlo, N. J. (2013) Aromatic-proline interactions: electronically tunable CH/ $\pi$  interactions, *Acc. Chem. Res.* 46, 1039-1049.
- (21) Pace, C. N., and Scholtz, J. M. (1998) A helix propensity scale based on experimental studies of peptides and proteins., *Biophys. J.* 75, 422-427.
- (22) Brown, A. M., and Zondlo, N. J. (2012) A Propensity Scale for Type II Polypyrrolone Helices (PPII): Aromatic Amino Acids in Proline-Rich Sequences Strongly Disfavor PPII Due to Proline-Aromatic Interactions., *Biochemistry* 51, 5041-5051.
- (23) Barlow, D. J., and Thornton, J. M. (1983) Ion-Pairs in Proteins., *J. Mol. Biol.* 168, 867-885.
- (24) Schreiber, G., and Fersht, A. R. (1996) Rapid, electrostatically assisted association of proteins., *Nat. Struct. Biol.* 3, 427-431.
- (25) Schreiber, G., Haran, G., and Zhou, H. X. (2009) Fundamental aspects of protein-protein association kinetics., *Chem. Rev.* 109, 839-860.
- (26) Hemsath, L., Dvorsky, R., Fiegen, D., Carlier, M. F., and Ahmadian, M. R. (2005) An electrostatic steering mechanism of Cdc42 recognition by Wiskott-Aldrich syndrome proteins., *Mol. Cell* 20, 313-324.
- (27) Blochliker, N., Xu, M., and Caflisch, A. (2015) Peptide binding to a PDZ domain by electrostatic steering via nonnative salt bridges., *Biophys. J.* 108, 2362-2370.
- (28) Li, X., Sutcliffe, M. J., Schwartz, T. W., and Dobson, C. M. (1992) Sequence-specific  $^1\text{H}$  NMR assignments and solution structure of bovine pancreatic polypeptide., *Biochemistry* 31, 1245-1253.
- (29) Su, J. Y., Hodges, R. S., and Kay, C. M. (1994) Effect of chain-length on the formation and stability of synthetic  $\alpha$ -helical coiled coils., *Biochemistry* 33, 15501-15510.
- (30) Litowski, J. R., and Hodges, R. S. (2001) Designing heterodimeric two-stranded  $\alpha$ -helical coiled-coils: the effect of chain length on protein folding, stability and specificity., *J. Pept. Res.* 58, 477-492.
- (31) Fletcher, J. M., Boyle, A. L., Bruning, M., Bartlett, G. J., Vincent, T. L., Zaccai, N. R., Armstrong, C. T., Bromley, E. H. C., Booth, P. J., Brady, R. L., Thomson, A. R., and Woolfson, D. N. (2012) A basis set of de novo coiled-coil peptide oligomers for rational protein design and synthetic biology., *ACS Synth. Biol.* 1, 240-250.
- (32) Fletcher, J. M., Harniman, R. L., Barnes, F. R. H., Boyle, A. L., Collins, A., Mantell, J., Sharp, T. H., Antognozzi, M., Booth, P. J., Linden, N., Miles, M. J., Sessions, R. B., Verkade, P., and Woolfson, D. N. (2013) Self-assembling cages from coiled-coil peptide modules., *Science* 340, 595-599.